Journal of Physics: Condensed Matter

PAPER

Unveiling spin-glass transition and antiferromagnetic order by μSR studies in spin-chain Sm_2BaNiO_5

To cite this article: A Indra *et al* 2019 *J. Phys.: Condens. Matter* **31** 165801

IOP Publishing Journal of Physics: Condensed Matter

J. Phys.: Condens. Matter 31 (2019) 165801 (7pp) https://doi.org/10.1088/1361-648X/ab01e6

Unveiling spin-glass transition and antiferromagnetic order by μSR studies in spin-chain Sm_2BaNiO_5

A Indra[1,2], K Dey[1,5], A Bhattacharyya[3], A Berlie[4] and S Giri[1]

[1] School of Physical Sciences, Indian Association for the Cultivation of Science, Jadavpur, Kolkata 700032, India

[2] Department of Physics, Srikrishna College, Bagula, Nadia, W. B., 741502, India

[3] Department of Physics, Ramakrishna Mission Vivekananda Educational and Research Institute, Belur Math, Howrah 711202, West Bengal, India

[4] ISIS Neutron and Muon Facility, Science and Technology Facilities Council, Chilton, Oxfordshire, OX11 0QX, United Kingdom

E-mail: sspsg2@iacs.res.in

Received 17 December 2018, revised 14 January 2019
Accepted for publication 24 January 2019
Published 20 February 2019

Abstract

We report the zero-field and longitudinal field muon spin relaxation studies in a spin-chain compound Sm_2BaNiO_5. Two magnetic transitions, that have not been previously detected by the heat capacity and magnetization measurements, are confirmed at 46 and 9 K. The antiferromagnetic order is suggested at 46 K. Analysis of the muon spin polarization unveils the spin-glass transition at 9 K. Time-field scaling relation of the muon spin polarization verifies the spin–spin autocorrelation function following the cut-off power law, which is approximated by the Ogielski form, as employed numerically for characterizing the spin-glasses.

Keywords: spin-glass, antiferromagnetic order, muon spin relaxation

(Some figures may appear in colour only in the online journal)

1. Introduction

Determination of the magnetic ground state is one of the crucial issues in magnetism. Specially, the absence of a long range magnetic order in association with the strong exchange interaction attracts the community. Studies of these systems with unusual ground states are at the forefront of condensed matter research [1–5]. Materials with the spin-glass (SG) ground state attract special attention for fundamental interests and technological applications [6–8]. Classically, magnetic frustration occurred due to competing ferromagnetic (FM) and antiferromagnetic (AFM) interactions associated with the disorder is set up for the SG ground state, where the absence of long range magnetic order has been realized, except for the reentrant spin-glasses (RSG). In the case of RSG, the SG state coexists with the long range magnetic order.

The R_2BaNiO_5 (R = rare earth) series of compounds crystallize in the orthorhombic structure with a *Immm* space group at room temperature [9]. Sm_2BaNiO_5 belonging to the R_2BaNiO_5 series holds a one dimensional (1D) spin-chain structure composed of Ni^{2+} ($S = 1$), as depicted in figure 1. The Ni atoms occupied at the center of NiO_6 octahedra form a chain-like structure along the crystallographic a-axis. The intra-chain Ni–Ni distance along a-axis is ~3.8062 Å, which is smaller than the Ni–Ni distances of 5.875 and 6.757 Å along b and c axes, respectively, at room temperature. The result provides a quasi one-dimensional (1D) spin-chain structure along a-axis for Sm_2BaNiO_5. Because of the 1D character several members of R_2BaNiO_5 series exhibit Haldane gap in the excitation spectrum [10–13]. The multiferroic order associated with a significant magnetoelectric coupling has been proposed in some members of the R_2BaNiO_5 series [14], such as Sm_2BaNiO_5

[5] Present address: Department of Physics, S.B.S.S. Mahavidyalaya, Goaltore, 721128, India

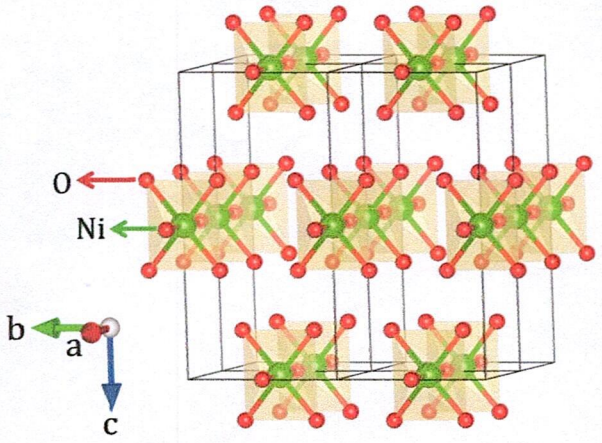

Figure 1. Array of NiO_6 chains along a-axis in Sm_2BaNiO_5.

[15], Dy_2BaNiO_5 [16], Tb_2BaNiO_5 [17], Er_2BaNiO_5 [18], Gd_2BaNiO_5 [19]. For Sm_2BaNiO_5 a structural transition to a non-centrosymmetric *Imm*2 space group from the centrosymmetric *Immm* space group has been proposed for interpreting the ferroelectricity above magnetic ordering temperature [15]. Preliminary magnetization studies were performed on Sm_2BaNiO_5, which revealed that the zero-field cooled magnetization exhibited a peak around 22 K along with a low temperature sharp upturn with further decreasing temperature. Low dimensional magnetic correlation has been proposed from the high resolution Fourier transform spectroscopy of Sm_2BaNiO_5 [20]. The Er^{3+} spectroscopic probe proposed that the magnetic moments of Sm_2BaNiO_5 in the ordered state were polarized along the crystallographic a axis [21]. Recently, the magnetic memory effects using various experimental protocols confirmed a cooperative glassy magnetic behavior below 9 K, although any definite signature of the glassy magnetic transition could not be detected from the bulk dc magnetization and ac susceptibility measurements for Sm_2BaNiO_5 [15].

Analogous to that observed glassy magnetic behavior of Sm_2BaNiO_5, the glassy magnetic or SG-like nature has been proposed at low temperature in some other members of the spin-chain compounds, R_2BaNiO_5 [15, 22–24]. In all the reported results of R_2BaNiO_5 series, any well defined glassy magnetic transition at low temperature could not be detected from the ac susceptibility, low-field dc magnetization, and heat capacity results. The glassy magnetic behavior has been anticipated either from the experiment on memory effects or the strong frequency dependence of the ac susceptibilities at low temperature, remaining unsolved issue in the low temperature glassy magnetic state. In addition, the AFM ordering temperature could not be confirmed for Sm_2BaNiO_5, because any well defined signature was absent in the magnetization and heat capacity results [15]. In order to establish a magnetic ground state, the powerful microscopic experiments using neutron scattering, nuclear magnetic resonance (NMR), and muon spin relaxation (μSR) need to be explored. Since the absorption cross-sections are too high to use neutron diffraction techniques for Sm and the difficulties of NMR studies in the ordered state, the μSR studies are useful to probe the low temperature ground state microscopically [25–32]. In the current investigation, we report the detailed results of our μSR studies of Sm_2BaNiO_5, recorded in zero-field and longitudinal field (LF) over a wide temperature range of 1.5–300 K. The analysis of the μSR results unveils a well defined SG transition at 9 K. Scaling of muon spin polarization decay with time and analysis of the dynamic relaxation process display similar characteristics, as reported for the classical spin-glasses [25, 26, 33–35]. We also observe an apparent signature of magnetic order at 46 K. The entire μSR studies provide a microscopic insight on the nature of an AFM order coexisting with the SG state, proposing that Sm_2BaNiO_5 is a reentrant SG compound.

2. Experimental details and analysis

The polycrystalline Sm_2BaNiO_5 is prepared using a solid-state reaction [15]. The chemically single phase composition is confirmed by the x-ray diffraction studies at room temperature recorded in a PANalytical x-ray diffractometer (Model: X' Pert PRO) using Cu Kα radiation. The μSR data are recorded in the EMU spectrometer [36] at the ISIS Pulsed Neutron and Muon source, United Kingdom. The full width at half maxima (FWHM) of a single pulse structure is 70 ns. The sample is sealed inside a silver sample holder with a thin silver foil. The sample is cooled down to 1.2 K in a standard ^{4}He cryostat with the He-exchange gas.

The μSR experiment involves implanting an ensemble of the spin polarized positive muons into the sample and come to rest at the interstitial sites. Each muon precesses in the sum of the local field attributed to the local environment and decays into a positron and two neutrinos, typically with a mean lifetime (τ_μ) of 2.2 μs. If the internal field is homogeneously distributed, a coherent precession of the muon spin is expected with $\omega = \gamma_\mu H$, where H is the applied field, γ_μ ($= 2\pi \times 13.55$ MHz kOe^{-1}) is the gyromagnetic ratio of the muon, and ω is the precession frequency of the muon spin. Here, the positron emits preferentially in the direction of the muon spin at the time of decay, so that, detection of the decay of positrons allows to determine the evolution of the muon spin polarization. The asymmetry of the muon decay is calculated by; $A(t) = [N_F(t) - \alpha N_B(t)]/[N_F(t) + \alpha N_B(t)]$, where $N_B(t)$ and $N_F(t)$ are the number of counts of the detectors in the forward and backward positions, and α is a constant, as determined from the calibration measurements made in the normal state with a small 20 Oe transverse applied magnetic field. The data are analyzed using the WiMDA software package [37].

In case of occurrence of a long range magnetic order, a distribution of the local field appears around magnetic phase transition and it fluctuates at a slow rate compared to the muon precession frequency. In such a case the muon spin relaxation or the decay of the ensemble of muon spin polarization $P(t)$ involves two relaxation mechanisms [38, 39]: (1) relaxation occurred due to dephasing of the muon spin precession for the inhomogeneous distribution and (2) relaxation ascribed to the thermal fluctuations of the local field. These are analogous to that observed inhomogeneous broadening

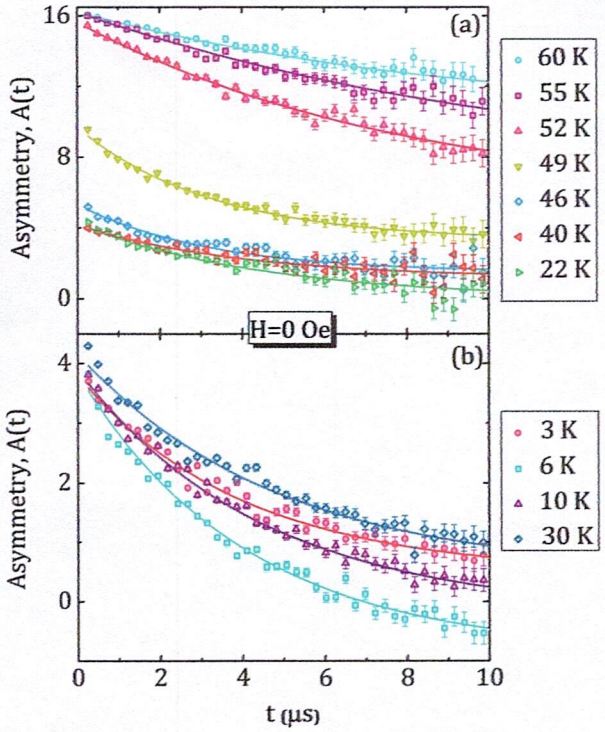

Figure 2. The muon asymmetry data with time at selected temperatures around (a) AFM magnetic order and (b) SG transition in zero field. Solid curves represent the fit using equation (3).

involving spin–spin relaxation mechanism and homogeneous spin-lattice relaxation mechanism of the NMR [40]. Thus $P(t)$ can be modeled as

$$P(t) = (1 - \eta_d)P_q(t) + \eta_d P_d(t). \quad (1)$$

First and second terms represent the relaxation processes involving dephasing of the muon spin precession for the inhomogeneous distribution and thermal fluctuations of the local field, respectively [41, 42]. η_d is the fraction of the initial muon spin polarization. In a randomly oriented powder sample $\eta_d = 1/3$ for time averaged local field, $\langle H_{\rm loc}\rangle >> \mu_0 H_{\rm L}$ and $\eta_d = 1$ for $\langle H_{\rm loc}\rangle << \mu_0 H_{\rm L}$, where $H_{\rm L}$ is the longitudinal magnetic field. Here, the asymmetry data are used for the analysis, where the relaxation function is defined as

$$A(t) = A_0 P(t). \quad (2)$$

Here, A_0 is the initial asymmetry. The distribution of relaxation times occurred due to local inhomogeneity the term $P_d(t)$ in equation (1) is analyzed using a stretched exponential function as

$$P_d(t) = \exp[-(\lambda_d t)^{\beta}], \quad (3)$$

with the muon spin-lattice relaxation rate λ_d and β is a power of the stretched exponential function. For $\beta = 1$, equation (3) typically stands for an exponential function. In case of distribution of relaxation processes, β is <1 and it is related to the width of the distribution. The distribution is wider for smaller values of β.

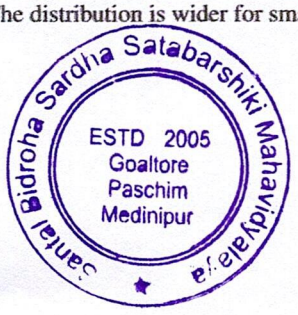

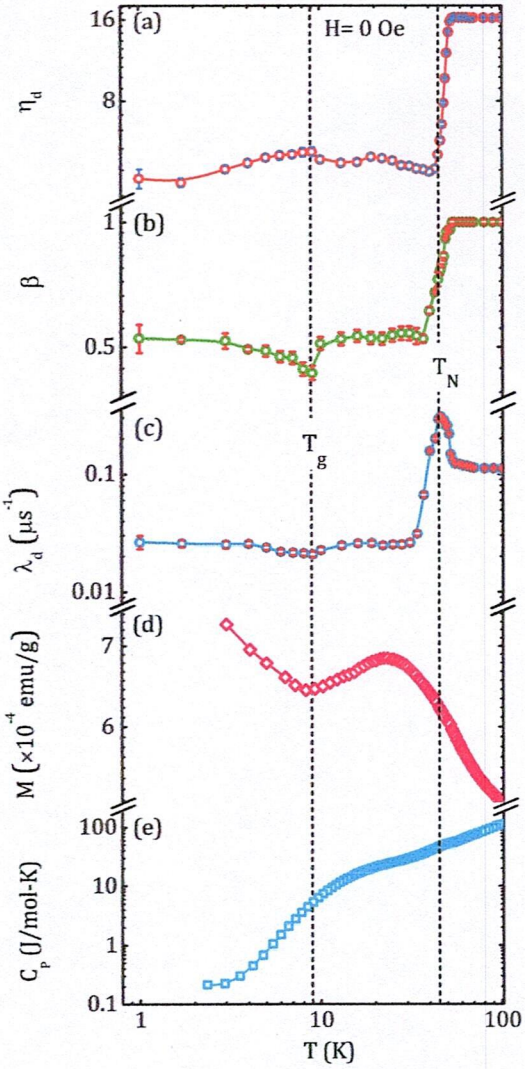

Figure 3. Temperature dependencies of the (a) fraction of the initial muon spin polarization, (b) stretched exponential power, (c) muon spin-lattice relaxation rate, (d) magnetization, and (e) specific heat capacity. Vertical broken straight lines depict temperatures of T_g and T_N, as described in the text. The M and C_P results in (d) and (e) are taken from [15].

3. Experimental results and discussions

3.1. Antiferromagnetic order

The zero-field μSR (ZF-μSR) measurements are recorded over a wide temperature range of 1.5–300 K, for which the sample is cooled in zero-field and ZF-μSR data are recorded at different temperatures. The ZF asymmetry data in the selected temperature (T) ranges are depicted in figures 2(a) and (b). Figure 2(a) shows the ZF asymmetry in the range of 22–60 K. In the paramagnetic state the signal is consistent with a weak depolarization of the muon signal, as depicted in figure 2(a) for $T \geqslant 55$ K. Below ~55 K, the muon signal changes rapidly and the initial muon polarization is strongly reduced. This happens due to a large distribution of the internal fields seen

Principal
S.B.S.S. Mahavidyalaya, Goaltore
Paschim Medinipur, Pin-721128

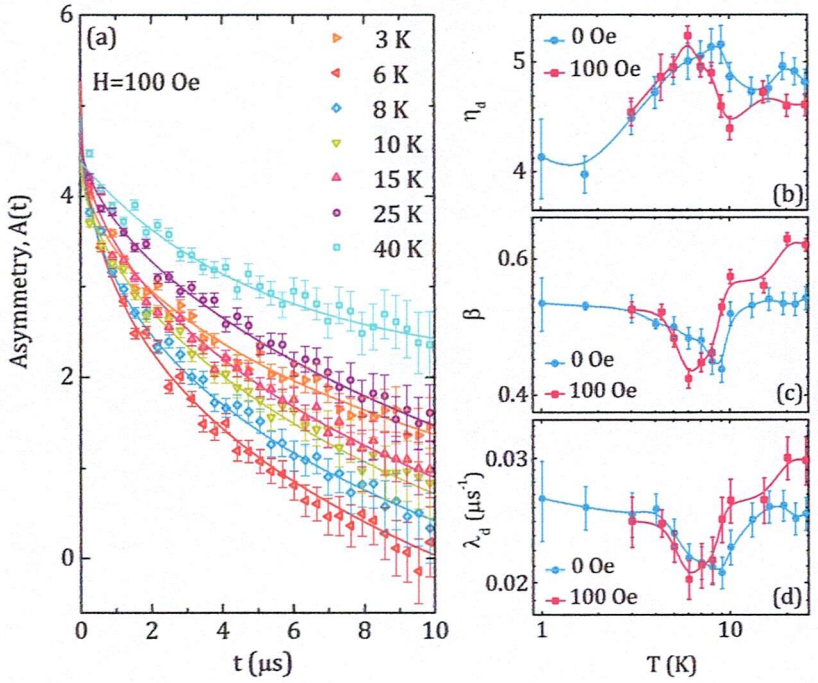

Figure 4. (a) Muon asymmetry data ($A(t)$) with time (t) at selected temperatures below T_N in presence of an LF of 100 Oe, where continuous curves show the fits using equation (3). Temperature dependence of (b) fraction of the initial muon spin polarization (η_d), (c) stretched exponential power (β), and (d) muon spin-lattice relaxation rate (λ_d) in zero and longitudinal field of 100 Oe.

by the μ^+. This probably emerges due to random distribution of the Sm and Ni moments in the lattice, while temperature approaches toward the magnetic ordering temperature. Figure 2(b) shows the ZF-μSR data in the low temperature range of 3–30 K. As depicted by the solid curves in figure 2, the muon asymmetry data are fitted using equation (3) considering that the stretched exponential relaxation function accounts for a continuous distribution of relaxation rates.

The fitted parameters as a function of temperature over the significant temperature regime of 1.5–100 K are depicted in figure 3. With decreasing temperature the value of η_d remains flat down to ~52 K. With further decreasing temperature the μSR signal is depolarized and the value of η_d starts to decrease rapidly, as depicted in figure 3(a). The value is close to 1/3 of the value in the paramagnetic state at ~46 K (T_N). In order to observe signature of true long-range magnetic order over a few lattice sites, a visible oscillation of the muon polarization should be noted at a well defined frequency. In the current observation the oscillation in the decay curve is missing. This oscillation may be absent due to the limited time resolution of a pulsed beam facility. Nevertheless, the μSR study confirms a magnetic order at 46 K, which could not be detected from the bulk magnetization and heat capacity results, as evident in figures 3(d) and (e), respectively [15]. Here, the magnetization and heat capacity results are given for the comparison and taken from our previous study [15]. We further note that the sharp fall of η_d takes place within 5 K of temperature interval, which is much smaller than observation close to the magnetic ordering temperature for AFM $NiGa_2S_4$ and isostructural $FeGa_2S_4$ [29, 30]. As shown in figure 3(b) the value of β is 1 in the paramagnetic state and it does not change down to ~52 K, below which β decreases sharply to 0.53 at ~35 K. Below 35 K the value of β is nearly flat, except for the temperature region around 9 K. The variation of $\lambda_d(T)$ is depicted in figure 3(c). A peak is observed at T_N in $\lambda_d(T)$, below which it behaves similarly to the thermal variation of β. Origin of the apparent signature at 9 K will be discussed later.

We note that the $\lambda_d(T)$ is nearly temperature independent down to ~70 K in the paramagnetic regime, as depicted in figure 3(c). This is often observed in a system with localized moments when thermal fluctuation energy is higher than the exchange energy between the spins [43]. In figure 3(c) the λ_d starts to increase slowly below ~70 K, which indicates signature of a short range magnetic order [44]. With further decreasing temperature a sharp increase of λ_d is observed, which appears due to the critical slowing down of the fluctuating moments while temperature approaches toward the magnetic order at ~46 K.

3.2. Spin-glass transition

The fitted parameters of $A(t)$ using equation (3) are depicted in figure 3 and exhibit an apparent hump like signature of an another transition at 9 K (T_g). At 9 K a maximum is observed in $\eta_d(T)$, whereas a minimum is observed in the $\beta(T)$ and $\lambda_d(T)$. The value of β decreases considerably at T_g, which becomes nearly temperature independent down to 1.5 K, except for the range of 3–10.5 K. The β-value is ~0.45 at T_g, which is close to that observed β-values at the spin freezing temperatures for $FeGa_2S_4$ [29] and $NiGa_2S_4$ [30]. The β value

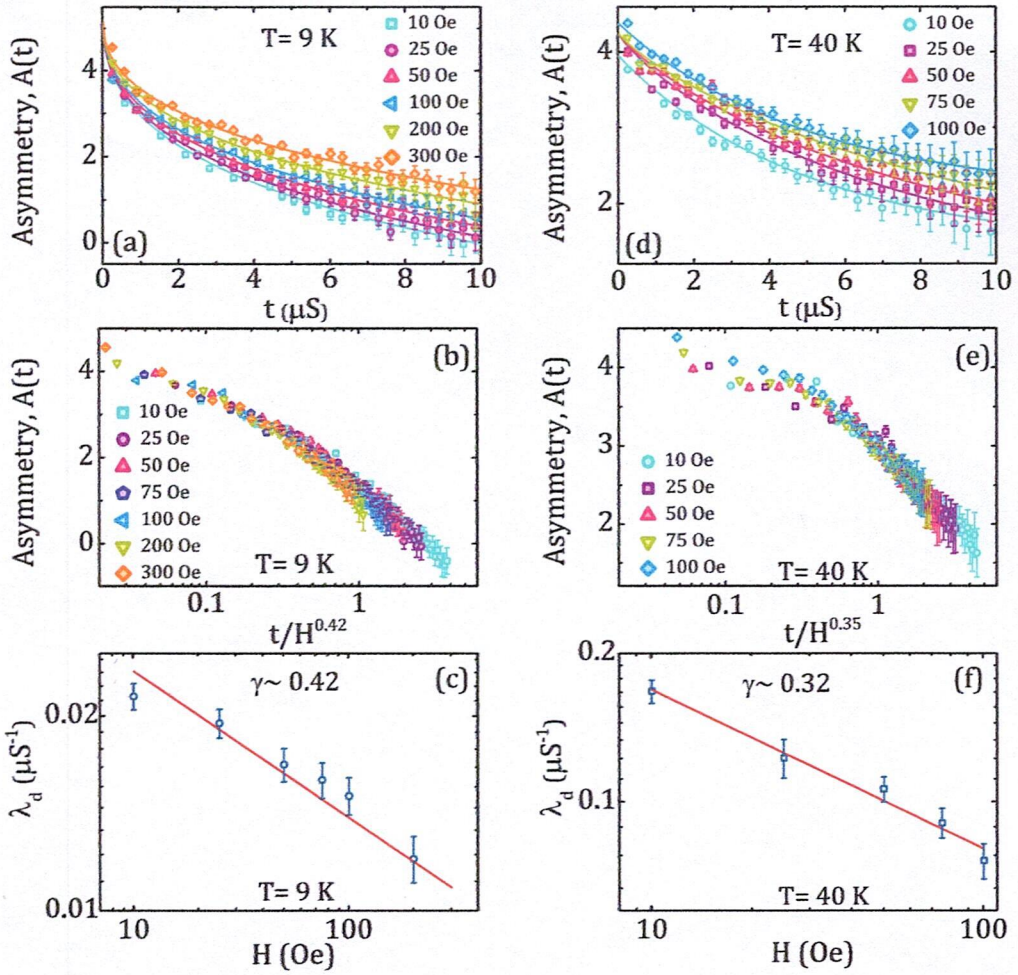

Figure 5. The muon asymmetry data with time at (a) 9 K and (d) 40 K at selected fields, where solid curves are the fits using equation (3). Scaled muon asymmetry data at different H with (b) $t/H^{0.42}$ at 9 K and (e) $t/H^{0.35}$ at 40 K in semi-log scale. The log–log plot of λ_d with H at (c) 9 K and (f) 40 K, providing the values of $\gamma = 0.42$ and 0.32, respectively from the linear fit.

has also been found close for $Pb(Fe_{1/2}Nb_{1/2})O_3$, where the SG state coexists with a magnetic order [45]. Similarly, the $\lambda_d(T)$ sharply decreases below T_N and becomes nearly temperature independent, except for the range of 4–10.5 K. Any signature of the vanishing λ_d-value is not observed in the temperature dependence, at least down to 1.5 K. Such existence of the strong spin-lattice relaxation dynamics is significant, which has been observed in the frustrated magnetic systems for both the cases of existent [29, 46–48] and non-existent long range magnetic order [30, 49–51]. Although the origin of which is not well understood, it indicates a zero-energy singularity in the density of excited states [46, 49, 52].

Below T_N, the longitudinal field μSR (LF-μSR) measurements are performed in an LF of 100 Oe over a temperature range of 1.5–40 K. Examples of LF-μSR spectra are depicted in figure 4(a) at selected temperatures. The LF spectra are also fitted using equation (3), as demonstrated by the solid curves in figure 4(a). The values of η_d, β, and λ_d with temperature, as obtained from the fits, are shown in figures 4(b)–(d), respectively and compared with the results of ZF spectra. As shown in the figure the signature of T_g is shifted toward lower temperature as a result of the longitudinal magnetic field of 100 Oe. The results are consistent with that observed shift of the spin freezing temperature toward low temperature due to the application of magnetic field for the disordered magnetic or SG systems [53, 54].

In case of second order phase transition the spin–spin dynamical autocorrelation function has been argued as $g(t) = \langle \vec{S}_i(t) \cdot \vec{S}_i(0) \rangle$, which can be described in general form as a cut off power law

$$g(t) \sim t^{-\alpha} f(t/\tau). \tag{4}$$

Here, i represents a site index, τ is a time scale that limits the upper range of the decay, α is the static and dynamic critical exponents, and the function, f is a cutoff function [55]. For $f(t/\tau) = 1$, equation (4) follows a power law [56]. Since muons are implanted in a sample initially in a fully polarized state and are depolarized in the nearest neighboring local magnetic moments, the form of the muon depolarization is correlated to the $g(t)$. In order to address the SG dynamics,

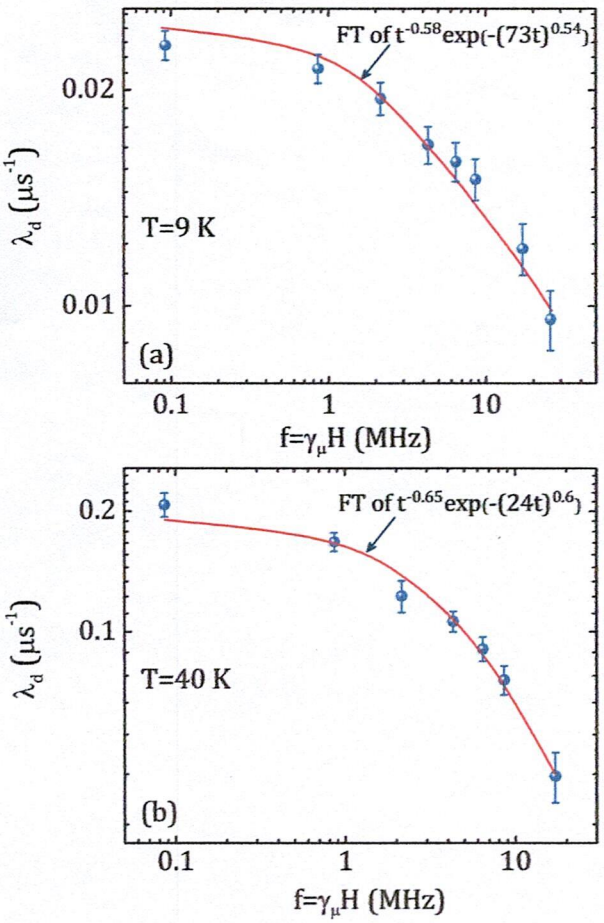

Figure 6. The log–log plots of λ_d with frequency, $f = \gamma_\mu H$ at (a) 9 K and (b) 40 K, where H is the field and γ_μ is the muon gyromagnetic ratio. Solid curves are the Fourier transform of the function described in the figures.

the muon depolarization has been discussed in detail by using the scaling relation

$$P(H,t) = P(t/H^{\gamma}), \tag{5}$$

where $\gamma = 1 - \alpha$ and this relation could be traced back to the correlation function given by equation (4) [25, 26, 33–35]. In the current investigation the μSR spectra are recorded at 9 K (T_g) and 40 K ($\sim 4.4T_g$) at different H. At 9 and 40 K the spectra at selected H are depicted in figures 5(a) and (d), respectively. Clearly, the H significantly influences the muon polarization, where the larger H provides weaker relaxation, pointing the decoupling effect. As depicted in figures 5(b) and (e), the scaling relation of equation (5) holds satisfactorily in the H-range of 10–300 Oe and 10–100 Oe at 9 and 40 K, respectively. Above these H-range, the muon polarization spectra do not follow the scaling relation satisfactorily. This may happen due to the fact that the electronic Zeeman energy at higher field dominates over the spin–spin coupling in the SG state. The spins are strongly polarized along the external field and SG frozen state is destroyed at high field. We note that the highest value of H following the scaling relation is higher at T_g (300 Oe) than the value (100 Oe) at $4.4T_g$. This indicates that the frozen state is destroyed at lower H, when the sample temperature moves away from T_g toward high temperature and approaches toward T_N. Here, the asymmetry spectra merge to a single curve for different H in figures 5(b) and (e) with the scaled value of $t/H^{0.42}$ and $t/H^{0.35}$ at 9 and 40 K, respectively. The values of γ are 0.42 and 0.35 at 9 and 40 K, respectively, which decreases with increasing temperature and is consistent with that observed in the classical SG systems such as in the diluted limit of Ag(Mn) using μ-SR studies [26] as well as Cu(Mn) and Au(Fe) using the neutron spin echo results [57]. The results are consistent with the Ogielski's simulations [58] and with the more recent results of Franzese and Coniglio [59]. We note that the conclusion is achieved in the current studies without assuming a specific functional form of the muon polarization.

Another complementary approach to satisfy the equation (5) is to fit the asymmetry data using equation (3), where the values of A_0 and β are kept fixed for different H. Here, the obtained values of λ_d for different H follow as $\lambda_d \propto H^{-\gamma}$. The log–log plots of λ_d with H at 9 and 40 K are depicted in figures 5(c) and (f), respectively. The linear fits of the plots are shown by the straight lines and provide the values of γ are 0.42 and 0.32 at 9 and 40 K, respectively, which are close to the values of γ, as obtained from the scaling relation given in equation (5). The magnetic field dependence of λ_d can also be further checked with the Ogielski form described as $\sim t^{-\alpha} \exp[-(\lambda_{OF} t)^{\beta_{OF}}]$, which has been numerically proposed for characterizing the spin-glasses [58]. Here, OF in the subscription represents the parameters following Ogielski form. The log–log plots of λ_d with f ($= \gamma_\mu H$) at 9 and 40 K are depicted in figures 6(a) and (b), respectively. The Fourier transform of $\sim t^{-\alpha} \exp[-(\lambda_{OF} t)^{\beta_{OF}}]$ at 9 and 40 K are depicted by the solid curves in figures 6(a) and (b), respectively. The reasonable fits give $\alpha = 0.58$ and 0.65, $\beta_{OF} = 0.54$ and 0.6, and $\lambda_{OF} = 73$ and 24 MHz at 9 and 40 K, respectively.

In summary, the ZF and LF-μSR studies confirm an AFM order at 46 K for Sm_2BaNiO_5. Well below T_N, a SG transition is revealed at 9 K, which is shifted toward low temperature by an LF of 100 Oe. Scaling of the time decay of muon polarization at 9 and 40 K for $\gamma < 1$, as defined in equation (5), follows the cut off power law approximated by the Ogielski form and proposes the SG behavior.

Acknowledgment

SG acknowledges the SERB proposal (SB/S2/CMP-029/2014), India for the financial support. The authors also thank the Department of Science and Technology, India (SR/NM/Z-07/2015) for the financial support for performing μSR studies at ISIS, United Kingdom and Jawaharlal Nehru Centre for Advanced Scientific Research (JNCASR) for managing the project (No. RB1768011). AB would like to acknowledge DST India, for Inspire Faculty Research Grant (DST/INSPIRE/04/2015/000169), and UK-India Newton funding for funding support.

ORCID iDs

S Giri https://orcid.org/0000-0002-1103-2601

References

[1] Ramirez A P 1994 *Ann. Rev. Mater. Sci.* **24** 453–80
[2] Lee P A 2008 *Science* **321** 1306
[3] Balents L 2010 *Nature* **464** 199
[4] Ramirez A P 2001 *Handbook of Magnetic Materials* vol 13, ed K H J Buschow (Amsterdam: Elsevier)
[5] Diep H T 2004 *Frustrated Spin Systems* (Singapore: World Scientific)
[6] Mydosh J A 1993 *Spin Glasses: an Experimental Introduction* (London: Taylor and Francis)
[7] Edwards S F and Anderson P W 1975 *J. Phys. F: Met. Phys.* **5** 965
[8] Binder K and Young A P 1986 *Rev. Mod. Phys.* **58** 801–976
[9] García-Matres E, Martínez J L and Rodríguez-Carvajal J 2001 *Eur. Phys. J.* B **24** 59–70
[10] Zheludev A, Tranquada J M, Vogt T and Buttrey D J 1996 *Phys. Rev.* B **54** 7210
[11] Zheludev A, Ressouche E, Maslov S, Yokoo T, Raymond S and Akimitsu J 1998 *Phys. Rev. Lett.* **80** 3630
[12] Zheludev A, Maslov S, Yokoo T, Raymond S, Nagler S E and Akimitsu J 2001 *J. Phys.: Condens. Matter* **13** R525
[13] Raymond S, Yokoo T, Zheludev A, Nagler S E, Wildes A and Akimitsu J 1999 *Phys. Rev. Lett.* **82** 2382
[14] García-Matres E, García-Muñoz J L, Martínez J L and Rodríguez-Carvajal J 1995 *J. Magn. Magn. Mater.* **149** 363–72
[15] Indra A, Dey K, Majumdar S, Sarkar I, Francoual S, Giri R P, Khan N, Mandal P and Giri S 2017 *Phys. Rev.* B **95** 094402
[16] Singh K, Basu T, Chowki S, Mahapotra N, Iyer K K, Paulose P L and Sampathkumaran E V 2013 *Phys. Rev.* B **88** 094438
[17] Upadhyay S K, Paulose P L and Sampathkumaran E V 2017 *Phys. Rev.* B **96** 014418
[18] Basu T *et al* 2014 *Sci. Rep.* **4** 5636
[19] Chowki S, Basu T, Singh K, Mohapatra N and Sampathkumaran E V 2014 *J. Appl. Phys.* **115** 214107
[20] Hadjiisldi Yu A, Paukov I V and Popova M N 1994 *Phys. Lett.* A **189** 109
[21] Klimin S A, Galkin A S and Popova M N 2012 *Phys. Lett.* A **376** 1861
[22] Basu T, Paulose P L, Iyer K K, Singh K, Mohapatra N, Chowki S, Gonde B and Sampathkumaran E V 2014 *J. Phys.: Condens. Matter* **26** 172202
[23] Basu T, Mohapatra N, Singh K and Sampathkumaran E V 2015 *AIP Adv.* **5** 037128
[24] Basu T, Singh K, Mohapatra N and Sampathkumaran E V 2014 *J. Appl. Phys.* **116** 114106
[25] Keren A, Mendels P, Campbell I A and Lord J S 1996 *Phys. Rev. Lett.* **77** 1386
[26] Keren A, Bazalitsky G, Campbell I and Lord J S 2001 *Phys. Rev.* B **64** 054403
[27] Petrakovskii G A, Aleksandrov K S, Bezmaternikh L N, Aplesnin S S, Roessli B, Semadeni F, Amato A, Baines C, Bartolomé J and Evangelisti M 2001 *Phys. Rev.* B **63** 184425
[28] Rovers M T, Kyriakou P P, Dabkowska H A, Luke G M, Larkin M I and Savici A T 2002 *Phys. Rev.* B **66** 174434
[29] Dalmas de Réotier P *et al* 2012 *Phys. Rev.* B **85** 140407
[30] Zhao S, Dalmas de Réotier P, Yaouanc A, MacLaughlin D E, Mackie J M, Bernal O O, Nambu Y, Higo T and Nakatsuji S 2012 *Phys. Rev.* B **86** 064435
[31] Calder S, Giblin S R, Parker D R, Deen P P, Ritter C, Stewart J R, Rols S and Fennell T 2013 *J. Phys.: Condens. Mater.* **25** 356002
[32] Guo H, Xing H, Tong J, Tao Q, Watanabe I and Xu Z-A 2014 *J. Phys.: Condens. Mater.* **26** 436002
[33] Keren A, Bazalitsky G, Mendels P, Campbell I and Lord J 2000 *Physica* B **289–90** 202
[34] Keren A and Bazalitsky G 2000 *Physica* B **289–90** 205
[35] Keren A, Gulener F, Campbell I, Bazalitsky G and Amato A 2002 *Phys. Rev. Lett.* **89** 107201
[36] Giblin S R *et al* 2014 *Nucl. Instrum. Methods Phys. Res.* A **751** 70
[37] Pratt F L 2000 *Physica* B **289–90** 710
[38] Schenck A 1985 *Muon Spin Rotation Spectroscopy: Principles and Applications in Solid State Physics* (Bristol: Hilger)
[39] Yaouanc A and Dalmas de Réotier P 2011 *Muon Spin Rotation, Relaxation, and Resonance: Applications to Condensed Matter* (*International Series of Monographs on Physics*) (New York: Oxford University Press)
[40] Slichter C P 1996 *Principles of Magnetic Resonance* (*Springer Series in Solid-State Sciences*) 3rd edn (New York: Springer)
[41] Kubo R and Toyabe T 1967 *Magnetic Resonance and Relaxation* ed R Blinc (Amsterdam: North-Holland) pp 810–23
[42] Hayano R S, Uemura Y J, Imazato J, Nishida N, Yamazaki T and Kubo R 1979 *Phys. Rev.* B **20** 850
[43] Moriya T 1956 *Prog. Theor. Phys.* **16** 23
[44] Ranjith K M, Majumder M, Baenitz M, Tsirlin A A and Nath R 2015 *Phys. Rev.* B **92** 024422
[45] Rotaru G M, Roessli B, Amato A, Gvasaliya S N, Mudry C, Lushnikov S G and Shaplygina T A 2009 *Phys. Rev.* B **79** 184430
[46] Yaouanc A, Dalmas de Réotier P, Glazkov V, Marin C, Bonville P, Hodges J A, Gubbens P C M, Sakarya S and Baines C 2005 *Phys. Rev. Lett.* **95** 047203
[47] Dalmas de Réotier P *et al* 2006 *Phys. Rev. Lett.* **96** 127202
[48] Chapuis Y, Dalmas de Réotier P, Marin C, Yaouanc A, Forget A, Amato A and Baines C 2009 *Physica* B **404** 686
[49] Keren A, Uemura Y J, Luke G, Mendels P, Mekata M and Asano T 2000 *Phys. Rev. Lett.* **84** 3450
[50] Marcipar L, Ofer O, Keren A, Nytko E A, Nocera D G, Lee Y S, Helton J S and Baines C 2009 *Phys. Rev.* B **80** 132402
[51] Gardner J S, Gingras M J P and Greedan J E 2010 *Rev. Mod. Phys.* **82** 53
[52] Uemura Y J *et al* 1994 *Phys. Rev. Lett.* **73** 3306
[53] de Almeida J R L and Thouless D J 1978 *J. Phys.: A Math. Gen.* **11** 983
[54] Sharma A and Young A P 2010 *Phys. Rev.* E **81** 061115
[55] Hohenberg P C and Halperin B L 1977 *Rev. Mod. Phys.* **49** 435
[56] MacLaughlin D E, Gupta L C, Cooke D W, Heffner R H, Leon M and Schillaci M E 1983 *Phys. Rev. Lett.* **51** 927
[57] Pappas C, Mezei F, Ehlers G, Manuel P and Campbell I A 2003 *Phys. Rev.* B **68** 054431
[58] Ogielski A T 1985 *Phys. Rev.* B **32** 7384
[59] Franzese G and Coniglio A 1999 *Phys. Rev.* E **59** 6409

Principal
S.B.S.S. Mahavidyalaya, Goaltore
Paschim Medinipur, Pin-721128